Atomic and electronic structure transformations of silver nanoparticles under a rapid cooling conditions[1]

Iván Lobato[1], Justo Rojas[1,2,*], Carlos Landauro[2], Juan Torres[2]

[1] División de Materiales, Instituto Peruano de Energía Nuclear,
Av. Canadá Nº 1470, Lima 41, Peru
[2] Facultad de Ciencias Físicas, Universidad Nacional Mayor de San Marcos,
Av. Venezuela s/n, Lima 14, Perú

Resumen

La evolución estructural y dinámica de nanogotas de plata Ag_{2869} (4.4 nm de diámetro) en condiciones de enfriamiento rápido se ha estudiado mediante simulaciones con dinámica molecular y cálculos de la densidad electrónica de estados. La interacción de átomos de plata se modeliza mediante el potencial semiempírico tight-binding propuesto por Cleri y Rosato. El cálculo de las funciones de correlación par y la técnica de análisis de pares se utilizan para revelar la transición estructural en el proceso de solidificación. Se muestra que las nanopartículas de Ag evolucionan en diferentes nanoestructuras bajo diferentes procesos de enfriamiento. A una tasa de enfriamiento de 1.5625×10^{13} K s^{-1} las nanopartículas preservan una estructura cercana a la amorfa que presenta gran cantidad de pares 1551 y 1541 los cuales corresponden a la simetría icosaédrica. A una velocidad de enfriamiento más baja (1.5625×10^{12} K s^{-1}), las nanopartículas se transforman en una estructura cristalina similar que consiste principalmente de pares 1421 y 1422 que corresponden a las estructuras cúbicas centrada en las caras y hexagonal compacta, respectivamente. Las variaciones de la densidad electrónica de estados para las nanopartículas enfriadas mediante diferentes procesos son pequeñas, pero en correspondencia con los cambios estructurales.

Abstract

The structural evolution and dynamics of silver nanodrops Ag_{2869} (4.4 nm in diameter) under rapid cooling conditions have been studied by means of molecular dynamics simulations and electronic density of state calculations. The interaction of silver atoms is modelled by a tight-binding semiempirical interatomic potential proposed by Cleri and Rosato. The pair correlation functions and the pair analysis technique are used to reveal the structural transition in the process of solidification. It is shown that Ag nanoparticles evolve into different nanostructures under different cooling processes. At a cooling rate of 1.5625×10^{13} K s^{-1} the nanoparticles preserve an amorphous-like structure containing a large amount of 1551 and 1541 pairs which correspond to icosahedral symmetry. For a lower cooling rate (1.5625×10^{12} K s^{-1}), the nanoparticles transform into a crystal-like structure consisting mainly of 1421 and 1422 pairs which correspond to the face centred cubic and hexagonal close packed structures, respectively. The variations of the electronic density of states for the differently cooled nanoparticles are small, but in correspondence with the structural changes.

1. Introducción

The research in the field of nanoparticles is the basis for the development of nanotechnology [1,2]. This is mainly due to the possibility of modifying the physical properties of these systems through the control of the system size. Silver nanoparticles are particularly interesting because they have a number of exciting potential applications in various fields including electronics and biology [3]. It is also known that the structure of a material determines its properties. For instance, in bulk face centred cubic materials the formation of other structures is suppressed kinetically, whereas nanoparticles of the same materials exhibit different structural modifications such as icosahedral, decahedral and amorphous with a great variety of physical and chemical properties [2, 4, 5]. Thus, in order to understand the structure of metal nanoparticles, obtained from the liquid

[1] Publicado en J. Phys.: Condens Matter 21(2009) 055301

[*] Correspondencia autor: jrojas@ipen.gob.pe

phase, it is important to investigate their structural evolution during solidification under different conditions. Molecular dynamics (MD) simulations have proved to be among the most effective methods in the investigation (at the atomic level) of the properties of nanoparticles, which is difficult to carry out experimentally. In fact, the structural evolution during cooling of metallic nanoparticles was extensively studied employing MD [6-11]. For the case of silver nanoparticles one can find some works concerning, for instance, investigations of the most stable structures and the melting process of small silver clusters [12], as well as the superheating of Ag nanowires [5]. The freezing of silver clusters and nanowires has also been studied recently [13]. In such work the authors conclude that the final structure of Ag clusters of ~2.3 nm is a fcc polyhedron despite the different cooling rates employed. In contrast, the study of the cooling rate dependence of solidification microstructures of silver by Tian *et al.* [14] indicates that the cooling rate has a crucial effect on the silver structure of the s olid state. For this case, they find a critical cooling rate for crystal forming of $\sim 1.0 \times 10^{13}$ K s^{-1} . Baletto *et al.* [15] analysed the equilibrium structure and melting of some magic number Ag nanoparticles, concluding that for relatively large clusters the fcc polyhedron is the most stable. However, according to experimental results of Reinhard *et al.* [16], both icosahedral and fcc structures are observed in large (up to 10 nm in diameter) free Ag clusters produced with an inert-gas-aggregation source. Hence, details of thermal stability, melting and freezing temperature for nanosized nonequilibrium systems still remain unclear.

In this work, we investigate the structural transitions of silver nanoparticles during fast cooling. The structural changes have been simulated employing a tight-binding many-body potential. Furthermore, the possible changes of the electronic properties of silver nanoparticles at different temperatures were analysed by calculating the electronic density of states (DOS).

The paper is organized as follows. Section 2 is devoted to presenting the details of the MD simulations, the structural analysis, and the Hamiltonian model for the calculation of the DOS. The results and discussion are presented in section 3. Some concluding remarks are provided in section 4.

2. Model and method

2.1 Potential energy function

The Ag nanoparticles are simulated by MD methods employing the many-body potentials developed by Rosato [17] on the basis of the second-moment approximation to the tight-binding model (SMA-TB). In this framework, the band energy of an atom *i* in a given position is proportional to the square root of the second moment of the local density of states. The energy of this atom is then written as a sum of two terms:

$$E_{tot} = \sum_i (E_i^{band} + E_i^{rep}) \qquad (1)$$

where

$$E_i^{band} = -\{ \sum_{j;r_{i,j} \le r_c} \xi^2 exp[-2q(\frac{r_{i,j}}{r_0} - 1)]\}^{1/2}, \qquad (2)$$

with ξ an effective hopping integral, $r_{i,j}$, the distance between the atoms *i* and *j* , r_c the cut-off radius for the interaction, r_0 the first-neighbour distance, and *q* the distance dependence of the hopping integral. The second term in equation (1) is the repulsive energy of Born–Mayer type:

$$E_i^{rep} = \sum_{j;r_{i,j} \le r_c} A exp[-p(\frac{r_{i,j}}{r_0} - 1)], \qquad (3)$$

The model parameters (ξ, A, p, q) are fitted to the bulk properties of the metal. The cut-off distance of the atomic interaction is set between the second-and third-neighbour distances. The parameters used in the simulation are taken from [17]; i.e. $\xi = 1.178$, $A = 0.1028$, $p = 10.928$, $q = 3.139$.

2.2 Simulation process

The MD simulations of a silver nanoparticle are carried out for a cubic box without periodic boundary conditions, so that the nanoparticle surface is free. The equations of motion are integrated over time using a velocity Verlet algorithm. Energy conservation with an error less than 1×10^{-3} % was achieved with a time step of 6.4 fs. The almost spherical nanoparticle was prepared by cutting a spherical region of a desired radius from a big face centred cubic

crystal. We have considered silver nanoparticles of different sizes ranging from 147 atoms up to 2869 atoms, but the results presented here are for systems of 2869 atoms, Ag_{2869} , (in some cases we also present results for nanoparticles of 147 atoms, Ag_{147}). It is worth mentioning that 2869 (and 147) belong to the set of magic numbers for icosahedral symmetries [2].

In order to obtain an equilibrium liquid-like state for the nanoparticle, we start the simulation at 1500 K which is a temperature higher than the equilibrium melting temperature of the Ag_{2869} nanoparticle (T_{melt} = 975 K). The system is kept at this temperature for 105 time steps (640 ps). Six different quenching processes are then carried out. The overall cooling rate was controlled by changing the number of MD steps in each run. As our first cooling process we chose a slow one in which the system is cooled from a liquid state at 1500 K to a temperature of 300 K, employing 1.2×10^5 MD steps, which corresponds to a cooling rate of 1.5625×10^{12} K s^{-1} (the k 1 process). In the last one, a fast cooling process, we employ 1.2×10^4 MD steps, which corresponds to a cooling rate of 1.5625×10^{13} K s^{-1} (the k 2 process). It is worth mentioning that recently Chen et al [10] employed the same cooling rates (k 1 and k 2) to study the structure and dynamics of a gold nanoparticle of similar size (2112 atoms). Thus, we consider these two cooling rates as our extreme cases so that we can compare the results for the two nanoparticles. The other four cooling rates k were chosen such that k 1 < k < k 2. On cooling, the temperature was decreased to room temperature (300 K) in steps of T = 10 K. The internal energy and structural configurations are recorded during the simulation.

2.3 Structural analysis methods

The pair correlation function. The pair correlation function (PCF) g(*r*) has been widely used to describe the atomic structure in amorphous, liquid and crystalline states. This quantity is given by [18].

$$g(r) = \frac{\langle n_i(r, r + \Delta r) \rangle}{\rho 4\pi r^2 \Delta r}, \qquad (4)$$

where ρ is the atomic density (N/V), and n_i (r, $r + \Delta r$) is the average number of atoms within a spherical shell surrounded by r and $r + r$ around an arbitrary atom.

Pair analysis technique. The common neighbours analysis (CNA) technique, introduced by Honeycutt and Anderson [19], is a standard tool for the interpretation of molecular dynamics simulations of structural transformations. The local environment of a pair of atoms is characterized by a set of four indices (*i, j, k, m*). The first one indicates whether the pair of atoms are closer than a given cut-off distance r_c . In the present work r_c is chosen to be equal the semisum of the first-and second-nearest-neighbour distances in the perfect fcc Ag lattice, that is r_c = 0.35 nm. The second index *j* is the number of common neighbours of the two atoms, and the third one is the number of bonds between the common neighbours. The fourth index is added to provide a unique correspondence between number and diagrams [19]. For instance, the 1551 pairs characterize the icosahedral-like local structure whereas the 1421 and 1422 pairs represent the fcc-like and hcp-like local structures, respectively. Additionally, icosahedral and fcc systems with structural defects are characterized by the 1541 and 1431 pairs, respectively. Finally, it is worth mentioning that pairs are named as type I if i = 1 and type II otherwise.

Electronic structure. In order to calculate the electronic properties of silver nanoparticles we employ a tight-binding Hamiltonian given by

$$H = \sum_{\vec{R}} \sum_{\vec{R}'} |\vec{R}\rangle H_{R,R'} \langle \vec{R}'| \qquad (5)$$

where {| R> } is the orthonormal (atomic-like) basis set centred at the site R with one orbital s at each site. The matrix elements $H_{R,R'}$ are defined by

$$H_{R,R'} = \begin{cases} \varepsilon_0 & \text{if } \vec{R} = \vec{R}' \\ t_0 & \text{if } |\vec{R} - \vec{R}'| \leqslant r_c \\ 0 & \text{if } |\vec{R} - \vec{R}'| > r_c \end{cases} \qquad (6)$$

with ε_0 and t_0 as the on-site and hopping terms, respectively. R_c is the same parameter as was employed in the CNA technique (see above). The atomic positions { R}, known from the MD simulation (see section 2.3), are fixed for these calculations. A physically relevant quantity for the study of the electronic properties of the system under

study is the density of states projected on the atomic position R , also known as the local density of states (LDOS). This quantity can be determined from:

$$n_R(\varepsilon) = \lim_{\gamma \to 0} \left\{ -\frac{1}{\pi} \mathrm{Im}\ G_{R,R}(\varepsilon - i\gamma) \right\} \quad (7)$$

where $G_{R,R}(\varepsilon - i\gamma)$ is the diagonal element of the one-particle Green function $G = (\varepsilon - i\gamma - H)^{-1}$. The recursion procedure is a real-space technique for tridiagonalizing a symmetric (Hermitian) Hamiltonian such that G can be expressed as a continued fraction formed by the so-called recursion coefficients. Details of the recursion method can be found in [20]. It is worth mentioning that this procedure allows us to collect the LDOS in different ways. Considering that an atom in an fcc solid has 12 first neighbours, for the nanoparticle we sum all the LDOS corresponding to atoms with 12 neighbours within r_c (fcc-like DOS, FDOS). Thus, in a well ordered nanoparticle with fcc-like structure the FDOS will be the main contribution to the total DOS. In this way we can compare the structural and electronic changes during the transformation.

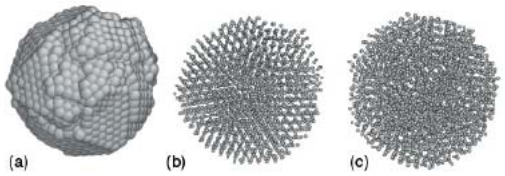

Figure 1. Atomic arrangements of the silver nanoparticle Ag_{2869} at 300 K cooled at rates of (parts (a) and (b)) 1.5625×10^{12} K s^{-1} and (part (c)) 1.5625×10^{13} K s^{-1} . The snapshots (a) and (b) correspond to the same configuration but different orientations. Visualization of atomic arrangements was done employing the AtomEye software [21].

3. Results and discussion

3.1 Atomic structure of silver nanoparticles

The nanoparticle Ag_{2869} is initially in the liquid state forming a nanodrop of approximately 4.4 nm diameter. As a result of quenching at different cooling rates we obtain, at 300 K, nanoparticles either in a crystal-like (cooling rate k 1 = 1.5625×10^{12} K s^{-1}) or a metallic glass (cooling rate k 2 = 1.5625×10^{13} K s^{-1}) structure, as illustrated qualitatively in figure 1. An imperfect nanocrystal with noticeable faceted morphology is obtained at a lower cooling rate (k 1), as shown in figures 1(a) and (b). At a fast cooling rate (k 2), nucleations of equilibrium phases are suppressed, and atoms exhibit random arrangements.

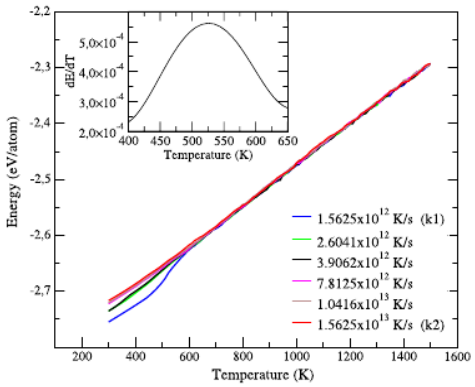

Figure 2. Caloric curves of the Ag_{2869} nanoparticle for various cooling rates. The curve of the fitted derivative dE/dT versus T for k 1 = 1.5625×10^{12} K s^{-1} is shown in the inset.

Figure 2 shows the variation of the average internal energy, E_t , as a function of temperature for various cooling rates. At a cooling rate of k 1 = 1.5625×10^{12} K s^{-1} the internal energy undergoes a sharp variation as the temperature decreases from approximately 600 to 500 K. As shown in the inset of figure 2, the transformation from liquid to crystal occurs over a wide temperature range (650–450 K): the peak of the heat capacity curve dE/dT, located at 527 K, is not sharp. On the other hand, at a cooling rate of k 2 = 1.5625×10^{13} K s^{-1} the caloric curve E_t has no inflection over the whole temperature range.

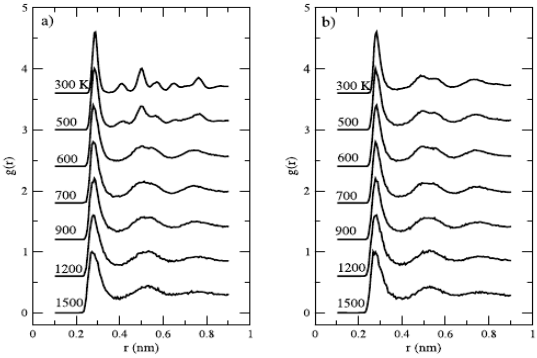

Figure 3. Pair correlation functions of the Ag_{2869} nanoparticle cooled at a rate of (a) 1.5625×10^{12} K s^{-1}, (b) 1.5625×10^{13} K s^{-1} .

The continuous change of the curve indicates that the system does not suffer structural changes; i.e. an amorphous solid is obtained in the undercooling state. The reason for this is that a high cooling rate restricts the atomic diffusion. This behaviour is very similar to that reported by Chen *et al* [10] for a gold nanoparticle of 2112 atoms.

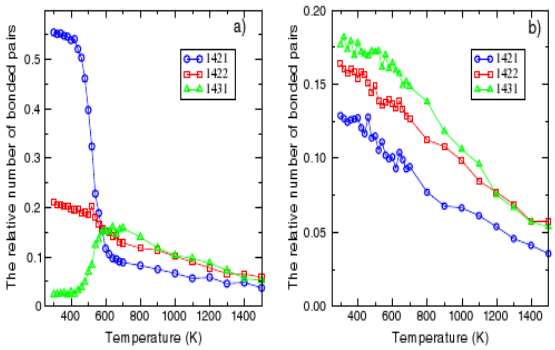

Figure 4. The relative numbers of bonded pairs 1421, 1422 and 1431 during freezing of the Ag_{2869} nanoparticle at cooling rates of (a) 1.5625×10^{12} K s^{-1}, (b) 1.5625×10^{13} K s^{-1}.

The critical cooling rate, *kc* , is the minimum value which is necessary for avoiding crystallization. For the nanoparticle Ag_{2869} we estimate *kc* from the analysis of the time evolution of the energy, E(t), as well as its temperature evolution, E(T) (see figure 2), and the corresponding PCFs g(r). Thus, we obtain the value of *kc* 7.8×10^{12} K s^{-1} . Although this value is close to that obtained for solid silver [14], kc depends on the size of the nanoparticle. It is also noticeable that the silver nanoglass, obtained at the cooling rate of 1.5625×10^{13} K s^{-1} , is very unstable. For instance, at room temperature after 6.4 ps the nanoglass transforms to the crystal-like structure in agreement with [13].

The changes in the atomic distribution within the nanoparticles, during the cooling process are extracted from the pair correlation function. Figure 3 shows the PCF at several temperatures and for the k 1 and k 2 cooling rates. First, in the temperature interval from 1500 to 600 K, we note for both cooling processes that the PCFs are identical, and reveal the typical structural features of an amorphous liquid with short-range topological ordering. At the cooling rate of 1.5625×10^{13} K s^{-1} the amorphous structure of the Ag_{2869} nanoparticle is conserved down to room temperature. As temperature decreases, it is clearly noticeable that there is a splitting of the second peak in the PCF, which is characteristic of amorphous structures [22]. On the other hand, the PCF of the Ag_{2869} nanoparticles cooled at a rate of 1.5625×10^{12} K s^{-1} below 500 K shows a typical structure corresponding to the fcc crystal.

More detailed information on the atomic structure in the nanoparticle can be obtained using CNA. At the liquid state onset (1500 K), the most abundant pairs are 1201 (21%), 1311 (21%), 1101 (12%), and 1422 (5.7%), for type I; and 2101, 2211 pairs, for type II. Figures 4 and 5 show the variations of the relative numbers of several principal bonded pairs versus temperature. Quantities are normalized such that the total numbers of pairs with i = 1 are unity. For temperatures above 650 K the number of principal pairs decreases slowly, but in the same proportion, after increasing the temperature, which occurs independently of the cooling processes (k 1 or k 2). This is an indication that the structure of the nanoparticle is not changing appreciably, which is in agreement with the PCF analysis (see figure 3). However, for temperatures below ~625 K the Ag_{2869} nanoparticle, cooled at a rate of 1.5625×10^{12} K s^{-1} , undergoes drastic structural changes.

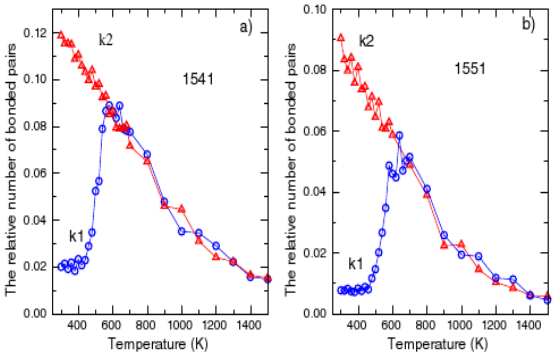

Figure 5. The relative numbers of bonded pairs in the Ag_{2869} nanoparticle: (a) 1541, (b) 1551. k 1 and k 2 are the cooling rates of 1.5625×10^{12} K s^{-1} and 1.5625×10^{13} K s^{-1} , respectively.

The number of 1421 pairs increases from 8% to 50% when the temperature decreases from 625 to 450 K, while the number of 1431 pairs, which represents defective fcc structure, practically falls to zero. Furthermore, the numbers of 1541 and 1551 bonded pairs increase equally, when

temperature decreases to 625 K, for both k 1 and k 2 cooling processes. Below this temperature the ratio of 1541 and 1551 pairs falls practically to zero for a relatively slow cooling rate of 1.5625×10^{12} K s^{-1} , while for a faster cooling process (e.g. k 2), the ratio of these pairs increases, reaching values of 12%, and 9% at room temperature, respectively (see figure 5). It seems that a low cooling rate allows the reorganization of the atomic order. As the present simulation reveals, the fcc crystalline silver nanoparticle of 4.4 nm size is more stable than an icosahedral one, which is consistent with the results of Baletto *et al.* [15]. These results are in good agreement with the CNA of a gold nanoparticle of 2112 atoms [10]. In the case of the small nanoparticle of 147 atoms the number of 1422 pairs, corresponding to hcp-like structures, increases to 35% (300 K) whereas the numbers of 1421 and 1551 pairs reach values of ~10% at room temperatures. In summary, for the small (147 atoms) and large (2869 atoms) nanoparticles, after the transition, the fcc-like and hcp-like structures predominate, respectively. A more detailed study of change as a function of the particle size is necessary in order to identify a possible threshold between different structures, as was reported in the case of Ni clusters by Qi *et al.* [6].

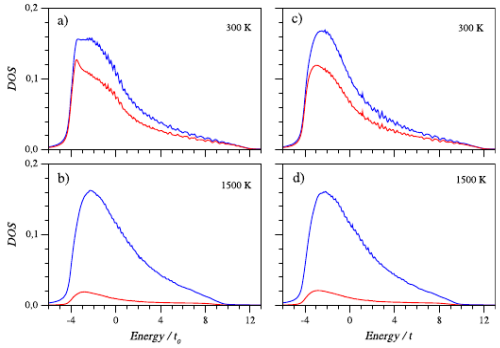

Figure 6. Total DOS (dark/blue lines) and FDOS (light/red lines) of the Ag_{2869} nanoparticle for two cooling rates: k 1 = 1.5625×10^{12} K s^{-1} ((a) and (b)) and k 2 = 1.5625×10^{13} K s^{-1} ((c) and (d)). The corresponding temperatures are indicated in the panels.

3.2. Electronic structure of silver nanoparticles

To determine the DOS of the silver nanoparticles we consider t_0 = 1 eV (reference energy), $\varepsilon_0 / t_0 = 0$, $\gamma / t_0 = 0.2$, ε / t_0 0.05 (energy step), and 75 (20) recursion coefficients for the Ag_{2869} (Ag_{147}) cluster.

Figure 6 shows the DOS of the Ag_{2869} nanoparticle for k 1 = 1.5625×10^{12} K s^{-1} and k 2 = 1.5625×10^{13} K s^{-1} for both initial (at 1500 K) and final (at 300 K) atomic configurations. Comparing the total DOS and the FDOS (fcc-like DOS) we can observe that at high temperatures the contribution of the FDOS to the total DOS is not remarkable.

This change completely at 300 K. For the k 1 cooling rate, the total DOS at room temperature is slightly more similar to the DOS of the fcc solid sample (not shown here), especially for the main peak at ~−3t_0 , which is not observed in the case for *k* 2. This should indicate, in agreement with the analysis of the atomic order (see section 3.1), that the silver nanoparticle with a slow cooling rate becomes more ordered (close to its solid counterpart) after decreasing the temperature. The differences in the total DOS, at room temperatures, for the two cooling rates are more appreciable for the small nanoparticle (Ag_{147}); see figure 7. For this case the FDOS is different from its fcc solid counterpart.

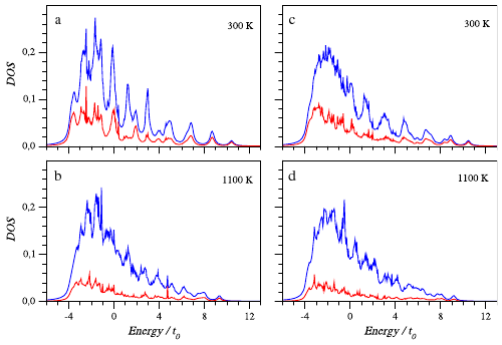

Figure 7. Total DOS (blue lines) and FDOS (red lines) of the Ag_{147} nanoparticle for two cooling rates: k 1 = 1.5625×10^{12} K s^{-1} ((a) and (b)) and k 2 = 1.5625×10^{13} K s^{-1} ((c) and (d)). The corresponding temperatures are indicated in the panels.

4. Conclusions

The glass formation and crystallization of a supercooled silver nanodrop, 4.4 nm in diameter, has been investigated on the basis of the MD simulation with the TB-SMA potential. The final structures are highly affected by the cooling rates. Ag_{2869} nanoparticles obtained in a supercooled liquid

with cooling rates higher than the critical value kc = 7.8×10^{12} K s^{-1} are very unstable metallic glasses, and nanoparticles resulting from relatively slow cooling rates are close packed crystals (fcc and hcp structures), as indicated by the CNA technique. At the cooling rate of 1.5625×10^{12} K s^{-1} we find a discontinuous structural transition near 527 K. The fully crystallized nanoparticle is a faceted polycrystal with a number of steps consisting of one atomic layer. The study of the evolution of the DOS with the temperature indicates that the electronic structure depends strongly on the size of the nanoparticle and the cooling rates.

5. Acknowledgment

The authors gratefully acknowledge the financial support of the CSI of the National University of San Marcos (Project N 081301061).

6. References

[1] Eberhardt W. Surf. Sci. 2002; 500:242.

[2] Baletto F, Ferrando R. Rev. Mod. Phys. 2005; 77:371.

[3] Shrivastava S, Bera T, Roy A. Nanotechnology. 2007; 18:225103.

[4] Gafner Yu, Gafner S, Entel P. Phys. Solid State. 2004; 46:1327.

[5] Shi DW, He LM, Kong LG, Lin H, Hong L. Modelling Simul. Mater. Sci. Eng. 2008; 16:025009.

[6] Qi Y, Cagin T, Johnson WL, Goddard W A III. J. Chem. Phys. 2001; 115:385.

[7] Baletto F, Mottet C, Ferrando R. Chem. Phys. Lett. 2002; 354:82.

[8] Nam HS, Hwang NM, Yu BD, Yoon JK. Phys. Rev. Lett. 2002; 89:275502.

[9] Shim JH, Lee SC, Lee BJ, Suh JY, Whan Cho Y. J. Cryst. Growth. 2003; 250:558.

[10] Chen Y, Bian X, Zhang J, Zhang Y, Wang L. Modelling Simul. Mater. Sci. Eng. 2004; 12:373.

[11] Delogu F. Nanotechnology. 2007; 18: 485710.

[12] Atis M, Aktas H, Guvenc Z. Modelling Simul. Mater. 2005; 13:1411.

[13] Qi WH, Wang MP, Liu FX, Yin ZM, Huang BY. Comput. Mater. Sci. 2008; 42:517.

[14] Tian ZA, Liu RS, Liu HR, Zheng CX, Hou ZY, Peng P. J. Non-Cryst. Solids. 2008; 354:3705.

[15] Baletto F, Ferrando R, Fortunelli A, Montalenti F, Mottet CJ. Chem. Phys. 2002; 16:3856.

[16] Reinhard D, Hall BD, Ugarte D, Monot R. Phys. Rev. B. 1997; 55:7868.

[17] Cleri F, Rosato V. Phys. Rev. B. 1993; 48:22.

[18] Stillinger FH, Weber TA. Phys. Rev. A. 1982; 25:978.

[19] Honeycutt JD, Andersen HC. J. Phys. Chem. 1978; 91:4950.

[20] Haydock R, Heine V, Kelly ML, Bullet DW. Solid State Phys. 1980: 35:215.

[21] Li J. Modelling Simul. Mater. Sci. Eng. 2003; 11:173.

[22] Li H, Wang G, Zhao J, Bian X. J. Chem. Phys. 2002; 116:10809.